Directional emissions achieved with anomalous reflection phases of metamaterials

Kun Ding,[1] Tao Jiang,[2] Jiaming Hao,[1] Lixin Ran,[2] and Lei Zhou[1,a)]
[1]*Surface Physics Laboratory (State Key Laboratory) and Department of Physics, Fudan University, Shanghai 200433, China*
[2]*The Electromagnetic Academy, Zhejiang University, Hangzhou 310027, China*

(Received 9 September 2009; accepted 9 December 2009; published online 28 January 2010)

For a small antenna placed on a metamaterial ground plane vertically or horizontally, we analyzed the conditions under which the antenna emissions are highly directional. We found through finite-difference time-domain (FDTD) simulations that a previously discovered directional emission phenomenon can be explained by our theory for the horizontal antenna case. For the vertical antenna case, we employed FDTD simulations to design a realistic metamaterial ground plane with desired reflection phase properties, and performed microwave experiments to verify its ability to support directional emissions. © *2010 American Institute of Physics*. [doi:10.1063/1.3289720]

I. INTRODUCTION

A directionally radiating antenna is highly desirable, in order to save unnecessary energy loss along unwanted radiation directions. A simple method is to put a ground plane on the back of an antenna to shield the backward radiations of the antenna. However, the ground plane has to be carefully designed to achieve a good functionality. For example, a metallic ground plane cannot work for an antenna put parallel to it since the radiation efficiency is low due to the destructive interferences between the source and the image formed by the ground plane. In addition, the directivity of the antenna on such a simple metallic plane is not good enough.[1]

Other approaches were proposed to manipulate the antenna's radiation pattern. For example, putting an antenna inside a Fabry–Pérot (FP) cavity,[2] in front of a photonic crystal (PhC),[3] or inside a PhC[4] can significantly modulate the radiation efficiency and directivity of the antenna. However, since a FP cavity and a PhC are all operated based on the Bragg mechanism,[5] such systems are typically bulky for microwave applications.

Recently, the development of artificial electromagnetic (EM) metamaterials has provided a platform for researchers to efficiently manipulate EM waves, resulting in several amazing EM phenomena possessing high application potentials, such as the invisible cloaking,[6,7] the super imaging,[8,9] and the polarization control.[10] In addition, metamaterials also stimulated the developments of several conceptual progresses in the fundamentals of the EM theory, with transformation optics as the most important example.[6] In recent years, several metamaterial-based approaches were proposed to enhance the radiation directivity and efficiency of an antenna.[11–15] For example, directional emissions can be achieved by simply putting a point source inside a zero-index metamaterial[11] or inside a subwavelength FP cavity formed by two specifically designed metamaterial reflectors.[12,13] However, similar to PhCs, such systems are still bulky and complex, which limit their applications in microwave technologies. Based on the concept of transformation optics, an antenna substrate has been designed to support high radiation directivity and efficiency.[16,17] However, the designed system possesses very complex permittivity and permeability distributions, making it difficult to realize in practice.[16,17]

In this paper, taking a single sheet of planar metamaterial as an antenna ground plane, we applied a dyadic Green's function (GF) approach to analytically study the radiation properties of small antennas put vertically or horizontally on the ground plane, and analyzed the conditions under which the antenna would radiate directionally and efficiently (Sec. II). We found that the metamaterial ground plane should exhibit certain incidence angle-dependent reflection phases in order to support directional emissions (Sec. II). Our theory can be employed to explain a previous experiment for the horizontal antenna geometry, and guides us to design a realistic structure to support directional emissions in the vertical antenna geometry, which is subsequently demonstrated by our experiments (Sec. III). We finally summarize our results in Section IV.

II. CONDITIONS TO ACHIEVE DIRECTIONAL EMISSIONS

As shown in Fig. 1(a), we consider a point dipole source put on top of a metamaterial substrate placed at the xy-plane (setting $z=0$). For simplicity, we assume that the current distribution of the point source is given by

$$\vec{J}(\vec{r},t) = \hat{\alpha}P_0\delta(\vec{r})e^{-i\omega_0 t}, \tag{1}$$

where ω_0 is the working frequency and $\hat{\alpha}$ is the polarization direction of the point source. From the frequency-domain Maxwell equations, $\nabla\times\vec{E}=i\omega_0\mu\vec{H}$, $\nabla\times\vec{H}=-i\omega_0\varepsilon\vec{E}+\vec{J}$, we find that the E field satisfies

$$[\nabla\times\nabla\times-\mu(\vec{r})\varepsilon(\vec{r})\omega_0^2]\vec{E}=i\omega_0\mu\vec{J}, \tag{2}$$

where $\mu(\vec{r})$, $\varepsilon(\vec{r})$ are the permeability and permittivity function of the system under study. Following Ref. 18, define a layered dyadic GF satisfying $[\nabla\times\nabla\times$

a)Author to whom correspondence should be addressed. Electronic mail: phzhou@fudan.edu.cn.

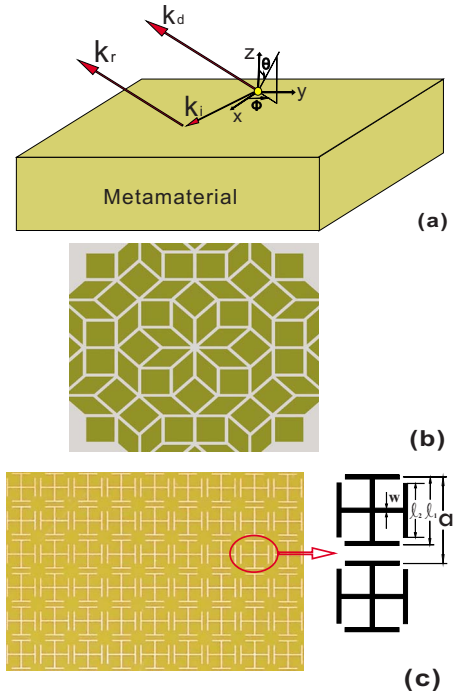

FIG. 1. (Color online) (a) Schematic picture of the system studied in this paper. (b) Schematic picture of the QC metamaterial substrate and all the structure parameters are the same as Ref. 14. (c) Picture of the metallic cross structure adopted experimentally, with inset showing the unit cell structural details:w=0.2 mm, a=7 mm, l_1=5.8 mm, and l_2=4 mm. The metallic cross structure is deposited on a 1.5 mm-thick dielectric substrate with ε_r =4.5.

$-\mu(\vec{r})\varepsilon(\vec{r})\omega_0^2]\overleftrightarrow{G}(\vec{r},\vec{r}';\omega_0)=\delta(\vec{r}-\vec{r}')\overleftrightarrow{I}$, it is easy to show that the E field radiated from the source described by Eq. (1) is rigorously given by

$$\vec{E}(\vec{r},\omega_0)=i\omega_0\mu_0 P_0\overleftrightarrow{G}(\vec{r},0;\omega_0)\cdot\hat{\alpha}. \tag{3}$$

The dyadic GF has been derived in Ref. 18. In the region $z>0$, we found that[18]

$$\overleftrightarrow{G}(\vec{r},0;\omega)=\frac{i}{8\pi^2}\int\frac{e^{i\vec{k}_\parallel\cdot\vec{r}_\parallel}\cdot e^{ik_z z}}{k_z}\times\begin{Bmatrix}\hat{e}(k_z)[\hat{e}(k_z)+R^{\mathrm{TE}}\hat{e}(-k_z)]\\+\hat{h}(k_z)[\hat{h}(k_z)+R^{\mathrm{TM}}\hat{h}(-k_z)]\end{Bmatrix}d\vec{k}_\parallel, \tag{4}$$

in which

$$\hat{e}(k_z)=\frac{k_y\hat{x}-k_x\hat{y}}{k_\parallel},\quad \hat{h}(k_z)=\frac{-k_z k_x\hat{x}-k_z k_y\hat{y}+k_\parallel^2\hat{z}}{k\cdot k_\parallel}, \tag{5}$$

and $k_\parallel^2+k_z^2\equiv k_x^2+k_y^2+k_z^2=(\omega_0/c)^2$, $R^{\mathrm{TE}}(\vec{k}_\parallel)$, $R^{\mathrm{TM}}(\vec{k}_\parallel)$ are the reflection coefficients for a transverse-electric (TE) or transverse-magnetic (TM) polarized plane EM wave with tangential wave-vector $\vec{k}_\parallel=k_x\hat{x}+k_y\hat{y}$.[19] Therefore, inserting Eq. (4) into Eq. (3), the entire E field distributions can be obtained. In what follows, we explicitly consider two examples.

We first consider the case that the small antenna is placed horizontally on the substrate surface. In such a case, put the antenna polarization $\hat{\alpha}=\hat{y}$ into Eq. (3), we obtain the **E** field distributions explicitly. In particular, on the H-plane surrounding the antenna (e.g., $y=0$), we find that

$$E_y(x,z;\omega)=-\frac{\mu_0\omega_0 P_0}{8\pi^2}\int\frac{e^{ik_x x}\cdot e^{ik_z z}}{k_z}\left\{\frac{k_x^2}{k_\parallel^2}[1+R^{\mathrm{TE}}(\vec{k}_\parallel)]+\frac{k_z^2k_y^2}{k^2k_\parallel^2}[1-R^{\mathrm{TM}}(\vec{k}_\parallel)]\right\}d\vec{k}_\parallel. \tag{6}$$

Generally, $R^{\mathrm{TE}}(\vec{k}_\parallel)$ and $R^{\mathrm{TM}}(\vec{k}_\parallel)$ are complex numbers, and can be rewritten as

$$R=|R|e^{i\varphi}, \tag{7}$$

where $|R|$ is reflection amplitude and φ is the reflection phase measured right on the air/metamaterial interface. In Eq. (7), we have omitted the subscripts TE and TM. We note expression (6) has very clear physical interpretations—each plane wave component radiated from the source interfere with the corresponding wave reflected by the substrate to form the entire field distribution of the antenna [see Fig. 1(a)]. Therefore, as long as the reflection properties (including both the amplitudes and phase changes for two polarizations) of the metamaterial substrate are known, the entire radiation pattern can be easily calculated.

To explore the physics embodied in Eq. (6), we further ignore the TM-mode components in the integrand in Eq. (6) since for this geometry the TM-components do not contribute too much to the **E** field on the H-plane. We found that Eq. (6) is simplified as

$$E_y(x,z;\omega)\approx-\frac{\mu_0\omega_0 P_0}{8\pi^2}\int\frac{e^{ik_x\cdot x+ik_z z}}{k_z}\frac{k_x^2}{k_\parallel^2}(1+|R^{\mathrm{TE}}|e^{i\varphi_{\mathrm{TE}}})d\vec{k}_\parallel, \tag{8}$$

which shows that the total field strongly depends on the reflection phase φ_{TE}. Specifically, if the reflection is in-phase ($\varphi_{\mathrm{TE}}=0°$), the constructive interference between the original and reflected beam leads to a maximized total **E** field; conversely if $\varphi_{\mathrm{TE}}=180°$, the total **E** field is minimized. Therefore, if φ_{TE} is sensitive to the incident angle θ, the radiation pattern will be strongly modified after reflections by the metamaterial. In particular, if we purposely design a metamaterial with a reflection phase function $\varphi_{\mathrm{TE}}(\theta)$ such that it approaches 0° for normally incident wave ($\theta=0°$) but goes quickly to 180° for slightly off-normal incidence angles, *an antenna put on top of such a metamaterial will radiate highly directionally*. Physically, this comes out because only the normal radiation survives due to the constructive interferences, and radiations along other angles are significantly suppressed due to the destructive interferences. Employing this idea, we can also achieve directional emissions along other particular directions (not necessarily the normal one) via designing metamaterials with appropriate reflection phase function $\varphi_{\mathrm{TE}}(\theta)$.

We now study the second case with the antenna put vertically on the metamaterial surface. In such a case, we find it natural to work with the **H** field. Put the antenna polarization $\hat{\alpha}=\hat{z}$ into Eq. (3), on the xy-plane setting $z=z_0=const.$, we find the **H** field is given by

$$\vec{H}(x,y;\omega) = -\frac{\omega_0 P_0}{8\pi^2\omega}\int \frac{e^{ik_x x}e^{ik_y y}e^{ik_z z_0}}{k_z}[1+|R^{\mathrm{TM}}|e^{i\varphi_{\mathrm{TM}}}](\hat{x}k_y - \hat{y}k_x)d\vec{k}_{\parallel}. \quad (9)$$

We found Eq. (9) is very similar to Eq. (8) except that here we need to consider the TM modes. Based on exactly the same arguments, we understand that the radiation pattern of a vertical antenna can be efficiently manipulated by the reflection phase function φ_{TM} of the substrate—the total radiation power is maximized (minimized) if φ_{TM} is 0° (180°). Therefore, again, we can purposely design an appropriate metamaterial to exhibit an incident angle sensitive reflection phase function φ_{TM} to make the antenna radiate directionally.

It is worth noting that we are primarily interested in the H-plane radiation properties of an antenna since the H-plane pattern shows no directivity for a free antenna without a ground plane. Therefore, in the horizontal antenna case, we are interested in the sensitivity of reflection phase to the incident angle θ; while in the vertical antenna case, we are more interested in the azimuth angle ϕ [see Fig. 1(a)].

III. PRACTICAL REALIZATIONS OF DIRECTIONAL EMISSIONS

In this section, we show that some metamaterials indeed possess the desired anomalous reflection phase properties, and we further demonstrate their abilities to support directional emissions.

A. Horizontal antenna case

We first consider the horizontal antenna case. In such a case, the metamaterial plate is required to exhibit a θ-sensitive reflection phase function $\varphi_{\mathrm{TE}}(\theta)$ for TE waves. Specifically, the ground plane should behave like a perfect magnetic conductor (PMC) for normally incident wave but change quickly to a perfect electric conductor (PEC) for waves with θ deviating from 0°. Interestingly, we found that a previously discovered directional emission phenomenon is just governed by this principle. In Ref. 14, it was shown that the radiation pattern of a small antenna put horizontally on a quasi-crystal (QC) metamaterial ground plane was highly directional. Although FDTD simulations were performed in Ref. 14 to explain the experimental results, the inherent physics for such an intriguing phenomenon was not clearly illuminated in Ref. 14. Here, we show that such a directional emission can be well explained by the present theory.

The structure studied in Ref. 14 is replotted in Fig. 1(b) schematically, which consists of a planar metallic patch array arranged in an eightfold QC pattern and a solid metallic sheet, separated by a thin dielectric layer (with ε_r=2.2) of a thickness 1.6 mm. We first performed FDTD simulations[20] to reproduce the FDTD results recorded in Ref. 14 and found that the radiation pattern of a dipole antenna put on top of this QC metamaterial substrate is indeed highly directional at frequencies around 7.5 GHz.[21] The FDTD calculated H-plane radiation pattern[20] of an 8 mm-long dipole antenna put on the QC substrate working at 7.5 GHz was depicted in Fig. 2(b) as (blue) stars, which are essentially the same as Fig. 4 of Ref. 14. To identify the directional emission mechanism, we studied the reflection phase properties of such a QC metamaterial at the frequency 7.5 GHz. Adopting the technique described in Ref. 22, we calculated the reflection phase φ_{TE} measured at the air/metamaterial interface, for TE-polarized plane waves with different incidence angles θ, and depicted φ_{TE} as a function of θ in Fig. 2(a) as (blue) stars. It is clear that φ_{TE} is very sensitive to θ, as expected. Simply speaking, the QC metamaterial substrate changes continuously from a PMC to a PEC when the incident angle varies from 0° to 90°. We found that the function $\varphi_{\mathrm{TE}}(\theta)$ can be well modeled by a Gaussian function

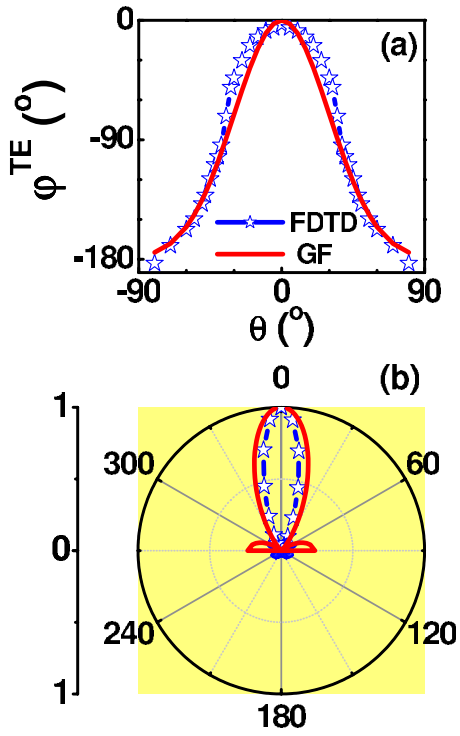

FIG. 2. (Color online) (a) Reflection phase φ^{TE}(in units of degrees) as a function of the incident angle θ (in units of degrees) with ϕ=0°, obtained by FDTD simulations with frequency setting f=7.5 GHz (blue open stars) and fitting with $\varphi^{\mathrm{TE}}(\theta)=180[\exp(-\theta^2/1800)-1]$ (red solid line). (b) Normalized H-plane radiation patterns of an 8 mm-long dipole antenna, obtained by the FDTD simulations (blue open stars) and GF method (red solid line), with frequency setting at f=7.5 GHz.

$$\varphi(\theta) = 180[\exp(-\theta^2/1800) - 1], \quad (10)$$

as shown by the solid line in the same figure. Put the reflection phase function Eq. (10) and $|R^{\mathrm{TE}}| \equiv 1$ into the GF formula Eq. (8), we calculated the **E** field distribution on the H-plane, and depicted the radiation pattern ($\propto|E|^2$) in Fig. 2(b) as a solid line. The radiation pattern calculated by the GF method is in good agreement with the FDTD calculations on the realistic sample, both exhibiting a sharp peak around θ=0°. Such agreements suggest that the directional emission found in Ref. 14 can indeed be explained by our theory.

This also provides us a hint to design other metamaterial substrates yielding directional emissions. Naturally, we need to have a periodic array of magnetic resonant structures to reflect EM waves in-phase for normal incidence case. Meanwhile, this resonance should not be so robust against varying the incidence angle θ. We found that a practical way to achieve this is to decrease the strength of the magnetic reso-

nance through, for example, replacing some resonant units by other nonresonant elements. In fact, if one looks carefully at the QC metamaterial structure [Fig. 1(b)], one may find that such a structure contains two different types of basic elements, namely, the metallic rhombus and the metallic square. These two elements yield different magnetic resonance frequencies. At the resonance frequency of rhombus elements (~7.5 GHz), square elements are nonresonant. As a result, the total strength of the magnetic resonance at this frequency is effectively decreased. At a large incidence angle, the behavior of the entire system would deviate significantly from a perfect magnetic mirror since the EM wave can "see" more nonmagnetic-resonant elements. This explains why the reflection phase of the QC metamaterial has such a strong dependence on the incidence angle (see Fig. 2(a)) at this frequency.

B. Vertical antenna case

We now consider the vertical antenna case. To achieve the directional emission in such a case, we need to have a ground plane exhibiting an anomalous φ_{TM} function, which is very sensitive to the azimuth angle ϕ of incident TM wave. The metamaterial that we found to possess such unusual reflection properties is a metallic cross structure,[23] with a real-sample picture shown in Fig. 1(c).

We first performed microwave experiments and FDTD simulations to investigate the radiation properties of a small antenna put vertically on such a ground plane. In our experiments, we fabricated a 497×497 mm^2 sample based on the design, and then put a monopole antenna vertically on the sample center, fed by a 50 Ω coaxial line passing through a small hole on the sample, which was connected to a network analyzer (Agilent 8722 ES). The radiation pattern was measured inside an anechoic chamber, using a receiver horn antenna placed at about 6 m away from the sample at a fixed angle θ. The sample was amounted on the stage, which can be rotated freely so that the azimuth angle ϕ can be changed. In our FDTD simulations,[20] we adopted a smaller plate sized 56×56 mm^2 due to the computational restrictions. The FDTD simulated and experimentally measured return loss ($|S_{11}|^2$) spectra are shown in Figs. 3(a) and 3(b), respectively, for a free antenna without ground plane (solid lines) and the antenna put on the ground plane (symbols). Comparison shows that the FDTD results are in reasonable agreements with the experimental results. In particular, the two dips in the experimental spectrum are also clearly identified in the FDTD spectrum, at similar frequencies. Since a dip in the return loss spectrum implies high antenna radiation efficiency, we then performed FDTD simulations to check the radiation patterns at these two S_{11} dip frequencies. FDTD calculations revealed that the lower S_{11} dip corresponds to the usual electric resonance of the cross structure, and the metamaterial just behaves as a good metal at this frequency. The radiation patterns calculated at this dip frequency were depicted in Figs. 4(a) and 4(b) (red circles), for H-plane and E-plane,[24] respectively, which were found quite similar to the

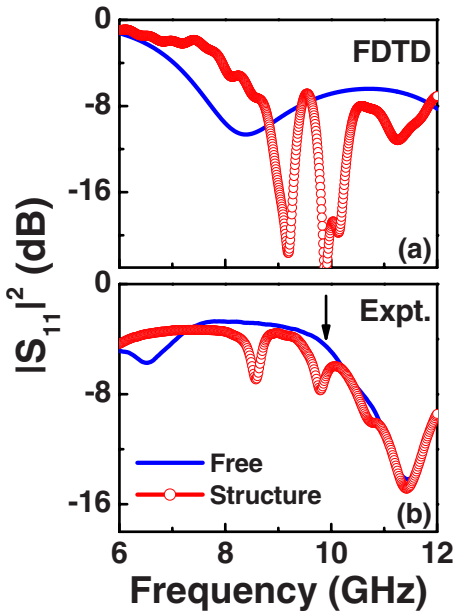

FIG. 3. (Color online) Return loss ($|S_{11}|^2$) spectra for a monopole antenna put vertically on the center of the substrate, obtained by (a) FDTD simulations and (b) experiments. The arrow in (b) represents the working frequency of the directional emission. The antenna adopted in our experiments is a modified monopole antenna so that its length is hard to determine accurately, while the antenna adopted in FDTD simulations is 6mm long.

patterns of the same antenna put on a metallic ground plane of the same size (black lines). Both cases do not show any directional emissions.[25]

However, around the second S_{11} dip, the radiation pattern is highly nontrivial. The radiation patterns at 10.04 GHz obtained by experiments (stars) and simulations (circles) are shown in Figs. 4(c) and 4(d) for H-plane and E-planes. First of all, we note that the experimental results are in excellent agreements with the FDTD results. Moreover, both experiments and simulations show that the radiation pattern for

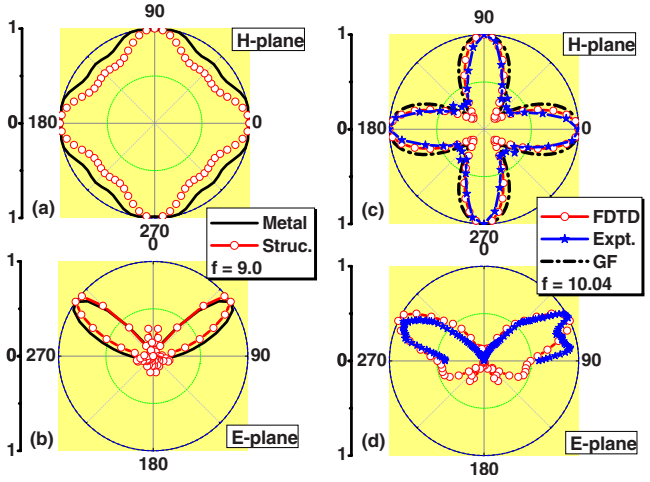

FIG. 4. (Color online) FDTD calculated normalized (a) H-plane and (b) E-plane radiation patterns of a 6 mm-long monopole antenna put vertically on our metamaterial substrate sized 56×56 mm^2 (circles) and on a metallic ground plane of the same size (lines), with frequency setting at 9.0 GHz. Normalized (c) H-plane and (d) E-plane radiation patterns of a monopole antenna put vertically on our metamaterial substrate, obtained by FDTD simulations (circles), experiments (stars), and the GF method (dashed-dotted lines), with frequency setting at 10.04 GHz.

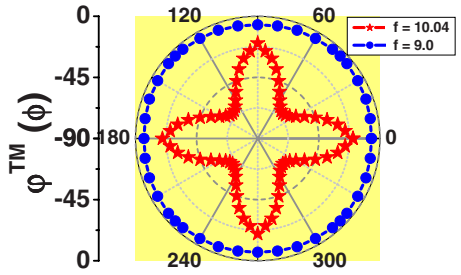

FIG. 5. (Color online) Reflection phase φ^{TM} (in units of degrees) as a function of the azimuth angle ϕ (in units of degrees) with $\theta=50°$, obtained by FDTD simulations at frequencies $f=10.04$ GHz (stars) and $f=9.0$ GHz (circles).

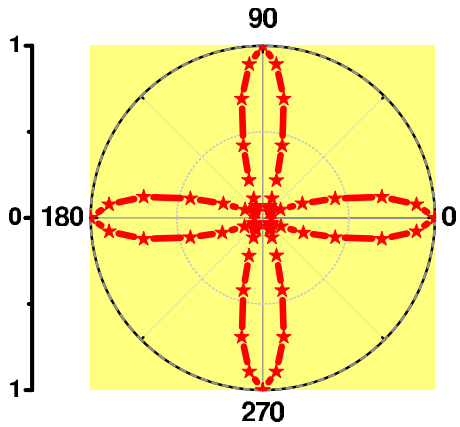

FIG. 6. (Color online) Normalized H-plane radiation pattern of a 6 mm-long monopole antenna put vertically on a modified metamaterial ground plane with structural details $w=0.5$ mm, $a=7$ mm, $l_1=5.5$ mm, and $l_2=4$ mm, obtained by FDTD simulations with frequency setting at 27.6 GHz. Here, we set $\theta=50°$ according to the E-plane result.

H-pane is quite directional, with four maximums appearing at $\phi=0°$ 90°, 180°, and 270° and four minimums in between these angles. This is quite intriguing at first sight since the system looks *isotropic* in the xy-plane [see Fig. 1(c)]. In fact, the system does behave like an isotropic PEC at the lower S_{11} dip frequency (although suffered from the shape anisotropy of the finite-sized ground plane).

Such an intriguing phenomenon can be easily understood from our theory. We employed FDTD simulations to calculate the reflection phase φ_{TM} of the TM-polarized plane wave incident on a metamaterial plate of an infinite size, as the function of the azimuth angle ϕ of the incident wavevector $\vec{k}$, with the frequency fixed at 10.04 GHz. Stars in Fig. 5 depict the calculated reflection phase φ_{TM} as a function of ϕ with θ fixed at 50°. From Fig. 5, we found that the reflection phase approaches to 0° when $\phi=0°$, 90° but changes quickly to −90° when ϕ changes from 0° to 45° (red stars). On the contrary, the FDTD simulated reflection phase function at the lower S_{11} dip frequency does not show any sensitivity to the angle ϕ (see blue circles in Fig. 5). The difference in reflection phases for $\phi=0°$ and 45° is caused by the mutual capacitance effects in the structure. When the incident **E** field is polarized along $\phi=45°$, two resonances corresponding separately to $E\hat{x}$ and $E\hat{y}$ will be excited simultaneously. We found that these two resonance modes have strong mutual capacitance effects at the frequency around 10 GHz, leading to a new resonance mode specific to $\phi=45°$. As a result, the system behaves highly anisotropic at this frequency. On the other hand, the mutual capacitance effect is negligible at frequency ~9 GHz, and therefore, the system behaves nearly isotropic at ~9 GHz (see Fig. 5).

Even though the reflection phase difference achieved by our structure between the two azimuth angles ($\phi=0°$ and $\phi=45°$) is not very big, such difference is already enough to make the radiation pattern rather directional. Putting the calculated reflection phase function $\varphi_{TM}(\phi)$ and $|R^{TM}|\equiv 1$ into our GF formalism Eq. (9) (the second case in Sec. II), we calculated the H-plane radiation pattern numerically, and depicted the pattern as a dashed-dotted line in Fig. 4(c). The GF results are in excellent agreements with both the FDTD and experimental results, all exhibiting radiation maximums at the same angles with similar widths. The excellent agreements among experiment, FDTD and GF methods have unambiguously demonstrated that the directional emission reported here is indeed governed by the anomalous reflection phase properties possessed by our metamaterial plate.

We emphasize here that the presently discovered directional emission is not a finite-size effect [in contrast to Fig. 4(a)]. We have checked the calculation results for larger and smaller plates and found essentially the same behaviors. On the other hand, the physics is dictated by the $\varphi_{TM}(\phi)$ function of the sample, which is an intrinsic property of the designed metamaterial ground plane.

The directivity of radiation can be enhanced by further optimization. For example, for a slightly modified structure, we showed in Fig. 6 the calculated H-plane radiation pattern at 27.6 GHz. The pattern showed that the directivity is much enhanced as compared with Fig. 4(c), with a half peak width only 25°. FDTD calculations demonstrate that the reflection phase $\varphi_{TM}(\phi)$ exhibits a stronger dependence on ϕ in this case.

IV. CONCLUSIONS

In conclusion, we have studied the radiation properties of a small antenna put horizontally or vertically on top of a metamaterial plate, and found the conditions under which the radiation would be highly directional. The key to achieve a directional emission is that the metamaterial plate should exhibit anomalous reflection phase that is sensitive to the incidence angles. We found that a previously discovered directional emission just belongs to the first case that we studied. For the vertical antenna case, we employed FDTD simulations to successfully design one such metamaterial sample and performed microwave experiments to demonstrate its ability to support directional emissions.

ACKNOWLEDGMENTS

This work was supported by the China-973 Program (Grant No. 2006CB921506), the NSFC (Grant Nos. 60725417, 60990321, 60531020, 60671003, 60701007), and NCET-07-0750 and Shanghai Science and Technology Committee (Grant No. 08dj1400302).

[1]J. A. Kong, *Electromagnetic wave theory* (EMW, Cambridge, 2000).
[2]T. Akalin, J. Danglot, O. Vanbesien, and D. Lippens, IEEE Microw. Wirel. Compon. Lett. **12**, 48 (2002).
[3]E. R. Brown, C. D. Parker, and E. Yablonovitch, J. Opt. Soc. Am. B **10**, 404 (1993).
[4]M. Thevenot, C. Cheype, A. Reineix, and B. Jecko, IEEE Trans. Microwave Theory Tech. **47**, 2115 (1999); B. Temelkuran, M. Bayindir, E. Ozbay, R. Biswas, M. M. Sigalas, G. Tuttle, and K. M. Ho, J. Appl. Phys. **87**, 603 (2000).
[5]E. Yablonovitch, Phys. Rev. Lett. **58**, 2059 (1987).
[6]U. Leonhardt, Science **312**, 1777 (2006); J. B. Pendry, D. Schurig, and D. R. Smith, *ibid.* **312**, 1780 (2006).
[7]D. Schurig, J. J. Mock, B. J. Justice, S. A. Cummer, J. B. Pendry, A. F. Starr, and D. R. Smith, Science **314**, 977 (2006).
[8]J. B. Pendry, Phys. Rev. Lett. **85**, 3966 (2000).
[9]A. Grbic and G. V. Eleftheriades, Phys. Rev. Lett. **92**, 117403 (2004); N. Fang, H. Lee, C. Sun, and X. Zhang, Science **308**, 534 (2005).
[10]J. M. Hao, Y. Yuan, L. X. Ran, T. Jiang, J. A. Kong, C. T. Chan, and L. Zhou, Phys. Rev. Lett. **99**, 063908 (2007); J. M. Hao and L. Zhou, Phys. Rev. B **77**, 094201 (2008); J. M. Hao, Q. J. Ren, Z. H. An, X. Q. Huang, Z. H. Chen, M. Qiu, and L. Zhou, Phys. Rev. A **80**, 023807 (2009).
[11]S. Enoch, G. Tayeb, P. Sabouroux, N. Guerin, and P. Vincent, Phys. Rev. Lett. **89**, 213902 (2002).
[12]L. Zhou, H. Q. Li, Y. Q. Qin, Z. Y. Wei, and C. T. Chan, Appl. Phys. Lett. **86**, 101101 (2005).
[13]A. Ourir, A. de Lustrac, and J.-M. Lourtioz, Appl. Phys. Lett. **88**, 084103 (2006).
[14]H. Li, Z. Hang, Y. Qin, Z. Wei, L. Zhou, Y. Zhang, H. Chen, and C. T. Chan, Appl. Phys. Lett. **86**, 121108 (2005).
[15]T. Jiang, Y. Sun, T. Li, W. Wang, W. Zhu, L. Peng, L. Ran, and J. Huangfu, Proceedings of the 2008 International Workshop on Metamaterials, 2008 , pp. 307–311.
[16]J. Zhang, Y. Luo, H. Chen, L. Ran, B.-I. Wu, and J. Au Kong, Prog. Electromagn. Res. **PIER 81**, 437 (2008).
[17]Z. Y. Duan, B.-I. Wu, J. A. Kong, F. M. Kong, and S. Xi, Prog. Electromagn. Res. **PIER 83**, 375 (2008).
[18]Y. Zhang, T. M. Grzegorczyk, and J. A. Kong, Electromagn. Waves **PIER 35**, 271 (2002).
[19]Note that $R^{\mathrm{TE}}(\vec{k}_{\parallel})$ is defined as $R^{\mathrm{TE}}(\vec{k}_{\parallel})=E_{\parallel}^{r}/E_{\parallel}^{\mathrm{in}}$ while $R^{\mathrm{TM}}(\vec{k}_{\parallel})$ is defined as $R^{\mathrm{TM}}(\vec{k}_{\parallel})=H_{\parallel}^{r}/H_{\parallel}^{\mathrm{in}}$, where "*r*" and "*in*" stand for reflected and incident waves.
[20]Simulations were performed using the package CONCERTO 4.0, developed by Vector Fields Ltd, England (2004). In our simulations, a basic cell sized $0.5\times0.5\times1.0$ mm^3 is adopted to discretize the space. Finer sub-meshes were adopted in space regions where strong inhomogeneity exists.
[21]Due to the computation limitations, the sample that we studied here is smaller than the experimentally adopted one,[14] and has a total size of 82×82 mm^2. However, the salient features obtained experimentally have all been reproduced by the FDTD simulations.
[22]L. Zhou, C. T. Chan, and P. Sheng, J. Phys. D: Appl. Phys. **37**, 368 (2004).
[23]J. Hao, L. Zhou, and C. T. Chan, Appl. Phys. A: Mater. Sci. Process. **87**, 281 (2007).
[24]It should be noted that since the E-plane pattern indicates that the maximum radiation appears at $\theta=50°$, we define our "H-plane" as the *xy*-plane with θ fixed at that particular value. The same definition strategy applies to Fig. 6.
[25]Apparently, the anisotropy in the radiation pattern is contributed by the shape anisotropy of the finite-sized ground plane.